Int. J. Pharm. Investigation, 2026; 16(4):1479-1488.
https://www.jpionline.org

Original Article

In silico Study toward Electronic Structures of Bioactive Compounds *Benzoquinone* and its Derivatives: Toxicity and Molecular Docking against Cyclin-Dependent Kinase

Israa Jameel Hakeem*

Department of Biological Sciences, College of Science, University of Jeddah, Jeddah, SAUDI ARABIA.

Correspondence:
Dr. Israa Jameel Hakeem
Department of Biological Sciences, College of Science, University of Jeddah, Jeddah-21589, SAUDI ARABIA.
Email: ijhakeem@uj.edu.sa; israajhakeem@gmail.com

Received: 26-03-2026;
Revised: 15-05-2026;
Accepted: 03-07-2026.

ABSTRACT

Background: Cyclin-Dependent Kinase is one of the important part the cell cycle control systems and normally active in breast cancer. DFT calculations, ADMET predictions and molecular docking on ligands such as compound 1 (*benzoquinone*), compound 2 (*naphthalene-1,4-dione*) and compound 3 (*2-isopropyl-5-methylcyclohexa-2,5-diene-1,4-dione*) assess their potential as *CDK4* inhibitors. **Objectives:** The purpose of this study was to assess *benzoquinone* and two derivatives as probable *CDK4* inhibitors using an integrated DFT, ADMET, and docking. It aimed to relate electronic reactivity and pharmacokinetic/toxicity profiles to binding affinity against *CDK4* Cyclin D3 (*CDK4* Cyclin D3) to line up the most hopeful prime compound. **Materials and Methods:** Here we optimized three drugs *benzoquinone, naphthalene-1,4-dione*, and *2-isopropyl-5-methylcyclohexa-2,5-diene-1,4-dione* using software Gaussian16 and functional B3LYP with basis set 6-311G(d,p). Molecular Docking and Pharmokinetics are studied using AutoDock Vina Discovery Studio Visualizer 4.0 and ADMETlab 2.0. **Results:** Frontier molecular orbital and DOS analyses showed that compound 3 with the smallest energy gap (3.71 eV) is predicted as the most reactive while compound 2 is more stable. MEP maps show that carbonyl oxygens are key reactive sites with compound 3 exhibiting the highest electronegative potential. ADMET analysis shows that compound 1 is found to be more soluble with strong BBB penetration, compound 2 displays strong CYP inhibition but higher toxicity risks, and compound 3 is more lipophilic with wider tissue distribution but poor CNS penetration. Docking studies against *CDK4*-Cyclin D3 (PDB ID: 7SJ3) showed compound 2 has the strongest binding affinity (-7.4 kcal/mol) while compound 3 displayed moderate binding and compound 1 the weakest. **Conclusion:** Molecular docking against the protein *CDK4*-Cyclin D3 predicted that compound 2 as the most promising candidate and also supported by the other studied results.

Keywords: *Cyclin-Dependent Kinase*, Drugs, FMO, DOS, Toxicity, ADMET, Molecular Docking.

INTRODUCTION

Cyclin-Dependent Kinases (CDKs) are a group of enzymes classified as serine/threonine kinases that are essential for controlling the progression of the cell cycle and regulating transcription in eukaryotic organisms (Malumbres *et al.*, 2009). Abnormal regulation or overactivity of CDKs is closely associated with the development of various cancers, which makes them significant targets for anticancer drug development (Asghar *et al.*, 2015). In current years, *in silico* approaches such as molecular docking, molecular dynamics simulations, and quantum chemical modeling have become appreciated tools in the initial phases of drug discovery. These methods assistance in exploring how possible inhibitors interact with CDKs, estimate binding strengths, and assistance to establish Structure Activity Relationships (SAR) (Azevedo, 2011; Solanki, 2023; Santos *et al.*, 2017).

Benzoquinone (i.e., *p*benzoquinone or 1,4benzoquinone) and its structural variations are organic molecules highlighting a conjugated diketone (quinone) framework that contributes to their diverse electronic and redox characteristics. These compounds are proficient of undergoing redox cycling, producing ROS (Reactive Oxygen Species), and forming covalent bonds through biological macromolecules; some derivatives also exhibit bioactivity (e.g., anticancer, antibacterial) or toxicity. For the reason that of their electronaccepting nature and redox reactivity, *benzoquinone* derivatives can oblige as hopeful primes in drug discovery while also posing safety apprehensions. Computational investigations of their molecular electronic properties including frontier orbital analysis, charge distribution, and reactivity descriptors, can offer valuable acumens into their chemical behaviour, stability, and

DOI: 10.5530/ijpi.20260027

likelihood of forming harmful reactive intermediates (White *et al*., 2025; El-Helw *et al*., 2024).

Quantum procedures, such as DFT (Density Functional Theory), are initial working to examine fundamental electronic properties such as HOMO-LUMO energy gaps, and Mulliken charge distributions which offer insights into the molecules' chemical reactivity and stability (Cristaldi *et al*., 2022; El-Helw *et al*., 2024; Kumar *et al*., 2025; Meng *et al*., 2011). These insights are then combined with molecular docking studies to evaluate how well the compounds interact with critical regions of the CDKs protein, including ATP-binding sites or another allosteric domain (Zheng *et al*., 2022). Perilous factors such as binding energy, hydrogen bonding patterns, hydrophobic contacts, and the overall compatibility of a ligand within the target proteins active site show a vivacious role in selecting effective drug candidates during molecular docking analyses (Ferreira *et al*., 2015; Li *et al*., 2025; Sofi *et al*., 2022). These molecular interactions make available early acumens into the inhibitory probable of compounds against specific targets like Cyclin-Dependent Kinases (CDKs). Moreover, computational ADMET (Absorption, Distribution, Metabolism, Excretion, and Toxicity) reporting supports to filter out molecules with poor pharmacokinetic appearances or safety concerns, permitting researchers to line up compounds with advanced therapeutic probable for further development (Abdelmonsef *et al*., 2024; Li *et al*., 2025).

This study presents an *in silico* workflow for appraising benzoquinone derivatives as probable CDK inhibitors. The procedure includes quantum chemical analysis for electronic properties, molecular docking to assess binding affinity, molecular dynamics simulations for complex stability, and ADMET predictions to assess safety. The goal line is to identify compounds with strong CDK-binding potential and acceptable pharmacokinetic outlines for future experimental validation.

MATERIALS AND METHODS

Computational Details

In the context of this study, we modelled three compounds: compound1(*benzoquinone*),compound2(*naphthalene-1,4-dione*), and compound 3 (*2-isopropyl-5-methylcyclohexa-2,5-diene-1,4-dione*) via GaussView 6.1 (Roy *et al*., 2016). The molecular geometries were improved with Gaussian 16 (Frisch *et al*., 2016), using the B3LYP hybrid functional (Lee *et al*., 1988; Becke *et al*., 1993) with the 6-311G (d,p) basis set (Frisch *et al*., 1984). This level of theory has been authenticated and effectively applied in prior studies (Sharma *et al*., 2025; Valarmathi *et al*., 2023). The Density of States (DOS) was made via GaussSum software (Allouche *et al*., 2012).

Molecular Docking

The crystal structures of the target proteins were retrieved from the Protein Data Bank (RCSB). The structure of the *CDK4*-Cyclin D3 complex bound to abemaciclib (PDB ID: 7SJ3) [https://www.rcsb.org/structure/7SJ3] was used in this study. *CDK4* is a cyclin-dependent kinases that play an essential role in regulating the G1 to S phase transition of the cell cycle, mainly through phosphorylation of the Retinoblastoma (Rb) protein. Their abnormal activation is commonly linked to uncontrolled cell proliferation and cancer development, making them well-established therapeutic targets.

Previously molecular docking, the receptor grid box was well-defined for precise binding site predictions. For PDB ID 7SJ3, the grid box was centred at x=17.905 Å, y=-37.699 Å, and z=3.299 Å. Docking was then executed via AutoDock Vina (Trott *et al*., 2009). The resulting ligand-protein interactions were more analysed and visualised with Discovery Studio Visualizer 4.0 (BIOVIA Systems, Dassault, 2021).

ADMET

For the ADMET assessment, we employed the ADMETlab 2.0 online server (https://admetmesh.scbdd.com) (Xiong *et al*., 2021; Zheng *et al*., 2022). ADMET, which stands for Absorption, Distribution, Metabolism, Excretion, and Toxicity, is a critical valuation in drug discovery as it makes available insights into the pharmacokinetic behaviour and probable safety of the compounds. These parameters can be predicted computationally and show how auspicious a compound might be as a drug candidate lacking experimental validation.

RESULTS

Optimization and Frontier Molecular Orbitals

To begin with, all three compounds were heightened, and their structures are shown in Figure 1A. Frontier Molecular Orbital (FMO) theory highlights the status of the HOMO and LUMO in governing a molecules chemical reactivity and interaction with other species. The energy gap between these orbitals influences stability, reactivity, and optical properties, with smaller gaps usually representing advanced reactivity (Krishna *et al*., 2024; Rezvan *et al*., 2025).

Figure 1B shows the frontier molecular orbitals (HOMO and LUMO) of the three compounds. The red and blue lobes represent the positive and negative phases of the molecular orbitals. For compound 1, the HOMO is at -7.59 eV and the LUMO at -3.73 eV, and the energy gap is 3.86 eV. Compound 2 shows a slightly smaller gap of 4.04 eV (HOMO at -7.42 eV and LUMO at -3.38 eV), while compound 3 has the narrowest gap of 3.71 eV (HOMO at -7.43 eV and LUMO at -3.72 eV). The HOMO-LUMO gap reflects the electronic excitation energy and provides insight into chemical reactivity and stability. A smaller gap generally suggests higher chemical reactivity and better charge-transfer ability, while a larger gap indicates greater stability and lower reactivity. Compound 3 appears to be the most reactive, whereas compound 2 is relatively more stable.

Density of States

Figure 2 shows the Density of States (DOS) spectra for the three compounds, where the HOMO and LUMO positions are clearly indicated along with their corresponding energy gaps. Compound 1 has a gap of 3.86 eV, compound 2 exhibits a slightly larger gap of 4.04 eV, and compound 3 shows the narrowest gap of 3.71 eV. The green and red vertical lines represent the occupied and virtual orbitals, while the blue line shows the overall DOS distribution.

These results are in promise with the FMOs, validating the stability and reactivity of the complexes. Compound 3 (with the narrowest gap) is more chemically predicted to be reactive and favourable for electronic transitions, whereas compound 2, taking the largest gap, demonstrates more electronic stability but reduced reactivity.

Molecular Electrostatic Potential Maps

The MEP maps of three compounds are revealed in Figure 3A. Each colour on these surfaces reveals electron density, thereby provided that information about probable reactive regions of the molecules. Red: High electron density regions (electrophilic positions); Blue: Low electron density areas (nucleophilic positions). Green areas resemble to a moderate electron density, a neutral part (Gu *et al*., 2024; Abuhejail *et al*., 2024).

For compound 1, the robust electron-rich regions are localised about the carbonyl oxygen atoms, signifying their role as probable positions for electrophilic interactions. In compound 2, the prolonged conjugated system spreads the electron distribution extra evenly, though the carbonyl groups still dominate as reactive centres. Compound 3 shows a similar trend, with oxygen atoms exhibiting high electron density, while the alkyl-substituted regions display comparatively electron-poor zones. The electronegative potential values for compound 1, compound 2, and compound 3, are -3.932 e^{-2}, -4.195 e^{-2}, and -4.865 respectively. MEP maps indicate that compound 3 possesses the highest electronegative potential compared to the other compounds.

Further, Mulliken charge distribution (Figure 3B) shows more negative partial charges on the oxygen centres, confirming the higher electron-withdrawing character of compound 3, and this aligns well with the MEP maps.

ADMET Analysis

Table 1 provides a comparative overview of the ADMET properties of the three compounds. All three molecules fall within a low molecular weight range (108-164 g/mol) and share similar structural features, with two hydrogen bond acceptors each and no hydrogen bond donors. Compounds 1 and 2 are each rigid, containing no rotatable bonds, whereas compound 3 contains one rotatable bond for slightly increased flexibility. The Topological Polar Surface Area (TPSA) values illustrate that 1 and 3 are moderately polar, whereas 2 is significantly non-polar. The solubility, compound 1 is less soluble (Log s -1.184) than compounds 2 and 3, which are more soluble, reflecting higher hydrophobicity, confirmed by Log P values (1.625 and 2.144). Permeability of all three compounds has similar Caco-2 and MDCK permeability, with 3rd compound being slightly higher, indicating good absorption potential. Distribution properties of all compounds showed high plasma binding (>88%), with compound 2 showing the greatest extent of plasma binding, and only a very low level of free drug is available in plasma. Compound 1 exhibits high BBB penetration (0.98), while compound 2 exhibits moderate BBB penetration (0.309) and negligible for compound 3 (0.032).

The metabolic profile indicated that compounds 2 and 3 are potent inhibitors for CYP1A2, CYP2C19, and CYP2D6 enzymes with higher potential to cause drug-drug interaction effects, while compound 1 shows negligible inhibition toward all the isozymes of cytochrome P450. As for elimination from the body, compounds 1 and 3 both display higher clearance (4.034 and 4.023), with compound 2 being less quickly eliminated, which is reflected in its short half-life (0.618 h). From above, compound 1 appears to be more water-soluble with good BBB penetration, compound 2 is metabolically active and with better CYP inhibition, whereas Compound 3 becomes lipophilic, having broad tissue distribution; however, poor CNS exposure.

The excretion results show that considerable differences do exist among the three compounds. Compound 1 has relatively high clearance (CL=4.034) and short half-life ($T_{1/2}$=0.931 hr), indicating that it was rapidly cleared from the body and would not accumulate in the circulation. Compound 2 had the lowest clearance (CL=3.209) and the shortest half-life time period ($T_{1/2}$=0.618 hr) (Table 1). This would indicate that, despite its slower clearance than compound 1, it is also metabolized and excreted more quickly, thereby leaving the system more rapidly. The overall clearance of compound 3 is almost the same compared to compound 1 (CL=4.023) and presents a half-life of 0.807 hr, indicating a rapid elimination profile, but with slightly longer retention than compound 1.

Toxicity Analysis

The toxicity of three compounds exhibits both similarities and differences (Table 2). All three reveal low hERG blocking activities and thus a reduced liability for cardiotoxicity. Regarding Hepatotoxicity (H-HT), compound 3 presents a little higher risk in evaluation to 1 and 2. Drug-Induced Liver Injury (DILI) is predicted to be most prominent for compound 2, while compounds 1 and 3 current lower probabilities. Mutagenicity, measured via AMES toxicity, is also main for compound 2, representing greater genotoxic risk, whereas compound 1 illustrations the lowest. Rat oral acute toxicity values are comparable across the compounds, shiny comparable levels of acute toxicity.

Table 1: Predicted ADMET properties of the compounds 1, 2 and 3.

ADME	Compound 1	Compound 2	Compound 3
MW	108.2	158.04	164.08
H-bond acceptors	2	2	2
H-bond donors	0	0	0
Rotatable bond	0	0	1
TPSA	34.14	2	34.14
Log S	-1.184	-2.783	-2.475
Log P	0.281	1.625	2.144
Caco-2 Permeability	-4.482	-4.529	-4.322
MDCK Permeability	2.2×10^{-6}	2×10^{-6}	2.7×10^{-6}
Pgp-inhibitor	0.0	0.003	0.143
Pgp-substrate	0.001	0.0	0.0
HIA	0.009	0.006	0.003
$F_{20\%}$	0.002	0.002	0.012
$F_{30\%}$	0.006	0.014	0.009
PPB	88.19%	91.81%	91.26%
VD	1.556	0.84	1.828
BBB Penetration	0.98	0.309	0.032
Fu	6.965%	2.229%	6.678%
CYP1A2 inhibitor	0.28	0.976	0.973
CYP2C19 inhibitor	0.088	0.578	0.79
CYP2C9 inhibitor	0.023	0.335	0.642
CYP2D6 inhibitor	0.001	0.109	0.875
CYP3A4 inhibitor	0.004	0.073	0.105
CL	4.034	3.209	4.023
$T_{1/2}$	0.931	0.618	0.807

Through reverence to drug safety, the FDA maximum daily dose (FDAMDD) predictions are favourable for all, though a little lower for compound 3. Skin sensitisation possibilities are high across all compounds, with compound 1 being slightly advanced. Carcinogenicity scores are close, with compound 2 show the highest tendency. Eye corrosion risk is maximum in compound 1, while compound 2 shows a much lower possibility. Though, all three compounds extant strong predictions for eye irritation, with values above 0.98. Respiratory toxicity seems to be more concerning for compounds 1 and 3, while compound 2 demonstrations comparatively lower risk.

Compound 2 appears as the least favourable in terms of liver toxicity, mutagenicity, and carcinogenicity, while compound 1, contempt being safer with reverence to mutagenicity and liver injury, illustrations higher chances of eye corrosion and respiratory toxicity. Compound 3 seems to be an intermediate with mild toxicity, but attention is drawn to hepatotoxicity and respiratory safety.

Molecular Docking

Docking of *CDK4*-Cyclin D3 complex bound to abemaciclib (7SJ3) with compound 1 (*benzoquinone*), compound 2 (*naphthalene-1,4-dione*), and compound 3 (*2-isopropyl-5-methylcyclohexa-2,5-diene-1,4-dione*). The docking scores of the three compounds in contradiction of the target protein (7SJ3) across nine different poses are concise in Table 3, providing a clear indication of their binding affinities. Compound 2 consistently shows the toughest binding across all poses, with the best docking score of -7.4 kcal/mol from pose 1 through pose 5, indicating a highly stable and favourable interaction. Compound 3 (docking scores of -6.8 to -5.7 kcal/mol across all nine poses) specified moderate and reasonable binding affinity. Conversely, Compound 1 exhibits the lowest interaction (between -5.7 and -4.3 kcal/mol for all the poses) that imitates lesser affinity.

Compound 1 was docked into the active site of the protein shown in Figure 4 (a). The ligand is stabilized by a series of non-covalent interactions, enhancing its affinity similarly to the orientation.

Particularly, it makes π-σ interactions with LEU A:147 (3.71 Å), and forms a π-alkyl contact with ALA A:33 (2.44 Å) while residues such as GLU A:94 (4.39 Å) are involved in van der Waals forces. These contacts contribute to the increased stability of the ligand-protein complex as a whole by reinforcing hydrophobic and dispersive interactions. The other surrounding residues VAL A: 20, ILE A: 12, PHE A: 93, and VAL A A:72 further stabilise the van der Waals interaction.

The interaction ranges are reasonable for efficient binding. Taken together, these stabilising effects suggest that the compound is well-positioned in the binding pocket and might contribute to its hypothesised biological activity.

The binding mode of the compound onto the active site residues of the target protein is shown in Figure 4 (b). The ligand is stabilised by hydrogen bonding and π-interactions. A conventional hydrogen bond, of the strong variety, formed with TRP A:179 at 2.20 Å that appears to stabilize it within the binding

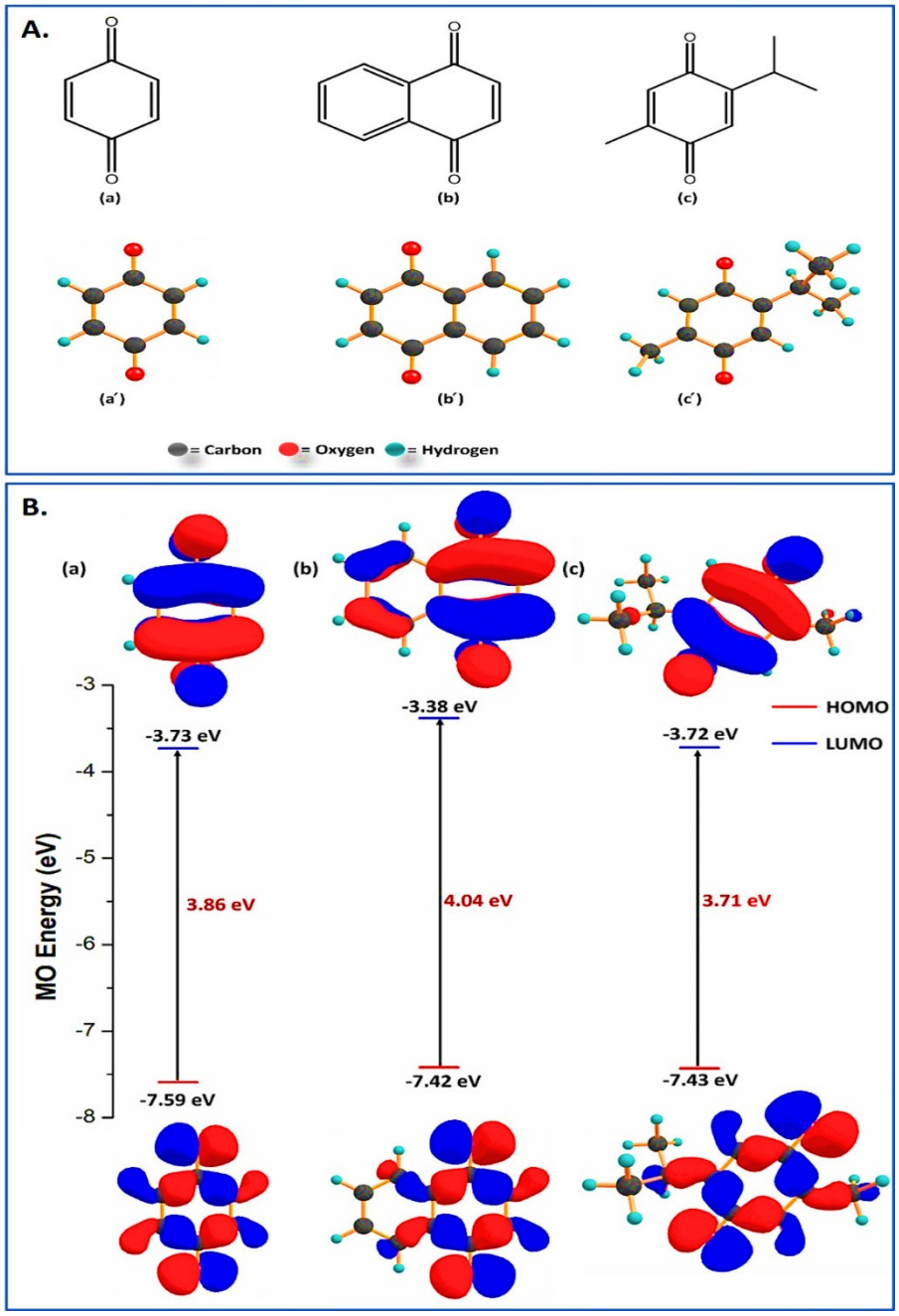

Figure 1: (A) ChemDraw and Optimized structures of compound 1 (a) and (a′) benzoquinone, compound 2 (b) and (b′) naphthalene-1,4-dione, and compound 3 (c) and (c′) 2-isopropyl-5-methylcyclohexa-2,5-diene-1,4-dione. (B) Frontier molecular orbital (HOMO-LUMO) distributions and corresponding energy gaps of the (a) compound 1; benzoquinone, (b) compound 2; naphthalene-1,4-dione, and (c) compound 3; 2-isopropyl-5-methylcyclohexa-2,5-diene-1,4-dione.

Table 2: Toxicity of Compounds 1, 2 and 3.

Toxicity	Compound 1	Compound 2	Compound 3
hERG blockers	0.004	0.015	0.006
H-HT	0.46	0.405	0.568
DILI	0.049	0.595	0.169
AMES Toxicity	0.131	0.831	0.314
Rat Oral Acute Toxicity	0.903	0.891	0.865
FDAMDD	0.883	0.853	0.833
Skin Sensitization	0.956	0.913	0.943
Carcinogenicity	0.775	0.821	0.805
Eye Corrosion	0.991	0.451	0.784
Eye Irritation	0.983	0.994	0.982
Respiratory Toxicity	0.98	0.571	0.965

Table 3: The binding affinity (kcal/mol) of quercetin and kaempferol ligands with receptors 7SJ3 is assessed through 9 different docking positions.

Docking Pose	Compound 1	Compound 2	Compound 3
Pose 1	-5.7	-7.4	-6.8
Pose 2	-5.7	-7.4	-6.8
Pose 3	-5.7	-7.4	-6.7
Pose 4	-5.7	-7.4	-6.6
Pose 5	-5.1	-7.4	-6.5
Pose 6	-5.1	-6.2	-6.4
Pose 7	-4.7	-6.0	-6.2
Pose 8	-4.4	-5.9	-6.2
Pose 9	-4.3	-5.7	-5.7

site. Furthermore, the aromatic ring of the ligand is involved in a π-π stacked interaction with TRP A:179 at 3.97 Å to enhance the binding affinity. Neighbouring residues LEU A:178, THR A:177, TYR A:180, LYS A:142 and GLU A:144 provide the hydrophobic and van der Waals environment and extra stability. Altogether, these interactions explain the accommodation of the compound in the protein pocket: TRP A:179 contributes to stacking and hydrophobic forces, while it interacts through hydrogen bonding

The binding interactions of the compound with residues in the active site of the protein are shown in Figure 4 (c). The ligand is stabilised by several non-covalent interactions. A typical hydrogen bond is found with HIS A:95 (2.79 Å) upon another one with VAL A:96 (2.20 Å), both being very important for fixing the ligand in place. The aromatic ring of the ligand is also involved in π-σ interaction with PHE A:93 (4.51 Å), and π-alkyl contacts with VAL A:20 (3.57 Å), which contribute to hydrophobic stabilisation. Other nearby residues, such as ILE A:12, ALA A:33, ALA A:157, VAL A:72 and LYS A:35, add van der Waals contacts to provide an optimum environment around the ligand in the binding pocket. All together these interactions indicate that the ligand is rigidly bound and hydrogen bonding and aromatic interaction are important in stabilising it.

DISCUSSION

Comparative study of three compounds: *benzoquinone* (compound 1), *naphthalene-1,4-dione* (compound 2) and *2-isopropyl-5-methylcyclohexa-2,5-diene-1,4-dione* (compound 3) in terms of their electronic structure, physicochemical and biological properties. FMO analysis indicates that the frontier orbitals are responsible for determining the reactivity of these molecules. The energy gap of compound 3 is the smallest (3.71 eV), indicating that it can easily undergo charge transfer and electronic excitation, which renders it much more chemically reactive than compounds 1 and 2. In contrast, 2 bearing the maximum gap energy (4.04 eV) appears to be more stable in electronic structure but less reactive toward charge-transfer (Abuhejail *et al*., 2024; Gu *et al*., 2024).

MEP maps are also corresponding to electron density distribution over the molecular surfaces (Abdelmonsef *et al*., 2024; Li *et al*., 2025). Carbonyl oxygen atoms in all three compounds were known as the most electron-rich centres, being the in sites for electrophile attack. But the red zones in compound 3 are sharper, which proposes a stronger electronegative probable and shares well with a smaller energy gap and advanced charge-transfer ability (Cavallo *et al*., 2016). The electronegative possible values

for compound 1, compound 2, and compound 3 are -3.932 e^{-2}, -4.195 e^{-2}, and -4.865 respectively. MEP maps indicate that compound 3 keeps the main electronegative possible compared to the other.

The ADMET analysis illustrations comprehensive information on the pharmacokinetic and physicochemical properties of the three compounds (Guan *et al*., 2018; Li *et al*., 2024). Compound 1 has the lowermost molecular weight and is most negative on Log S basis, exhibits high solubility, strong barrier penetration through the blood-brain barrier, appropriate for central nervous system use. Its low level of CYP inhibition and fast elimination also make it a safer candidate. Even if it is structurally rigid and metabolically active, compound 2 displays strong inhibition towards enzymes *CYP1A2, CYP2C19 and YP1A2*, compared to other non-competitive drugs, thus levitation the potentials of drug-drug interactions in patients. Also, its relatively poor solubility and high lipophilicity can preclude systemic absorption even if decent protein binding ensues. Compound 3 has an intermediate lipophilicity, while it is more broadly distributed in tissues, consistent with increased membrane permeation; still, its lack of BBB penetration may restrict potential CNS use. The total pharmacokinetic valuation of drug (compound 1) is more bioavailable and with lower toxicity, compound 2 is highly metabolically active but toxic and compound 3 is a lipophilic reactive compound ideal for other potential as its distribution property. These interpretations are confirmed via the toxicity assessment. All members exhibit low hERG block, revealing weak cardiotoxicity hazard. Nevertheless, compound 2 has the maximum scores of hepatotoxicity, mutagenicity and carcinogenicity, and all these outcomes showed momentous safety risks. Compound 1 is relatively safer in these respects but has a high chance of eye corrosion and respiratory irritation. Compound 3, with moderate hepatotoxicity and Compound 3, with moderate agree to take a safety balance correctly. This full

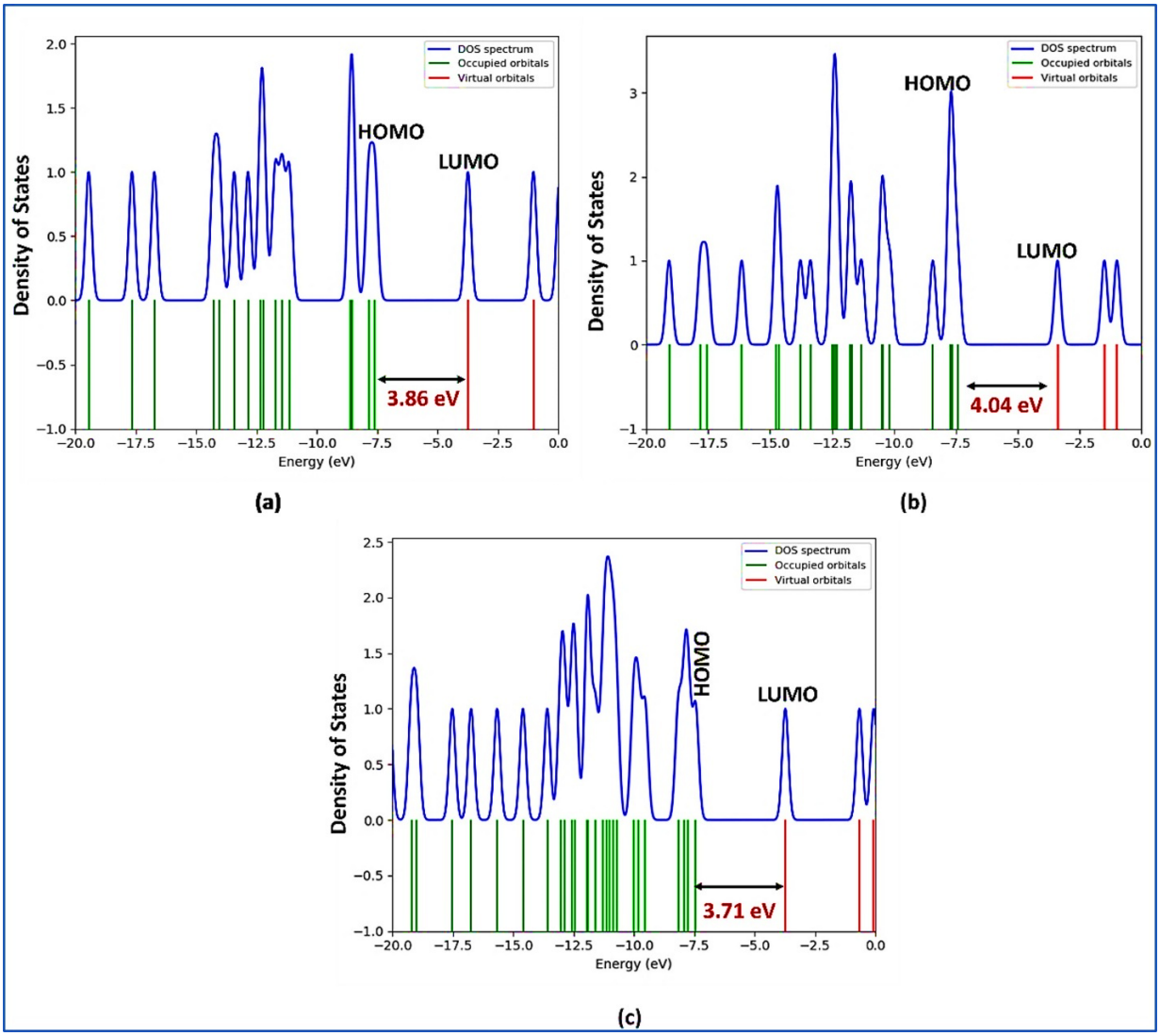

Figure 2: DOS plots of (a) compound 1; benzoquinone, (b) compound 2; naphthalene-1,4-dione, and (c) compound 3; 2-isopropyl-5-methylcyclohexa-2,5-diene-1,4-dione.

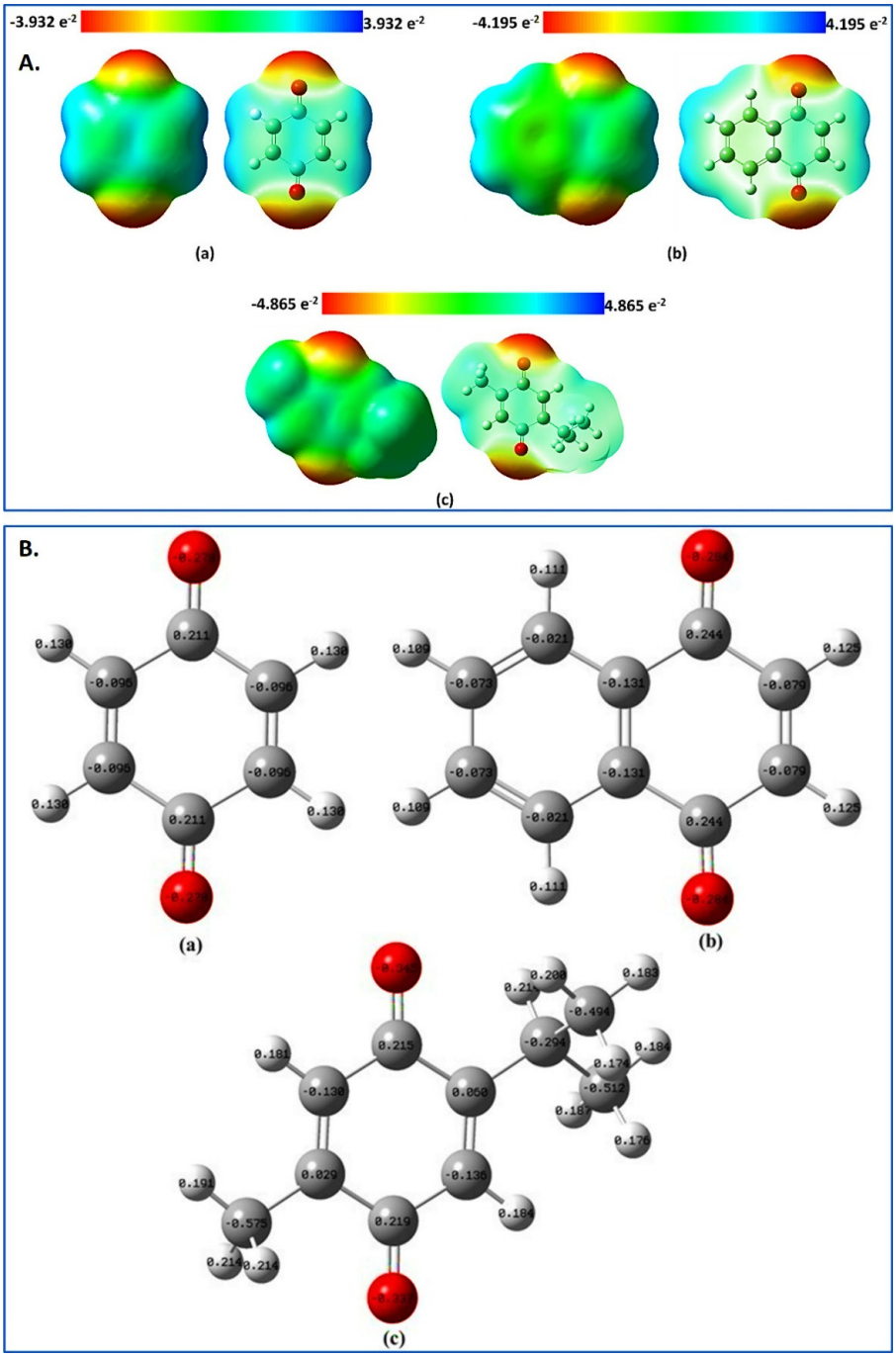

Figure 3: (A) MEP maps of (a) compound 1; benzoquinone, (b) compound 2; naphthalene-1,4-dione, and (c) compound 3; 2-isopropyl-5-methylcyclohexa-2,5-diene-1,4-dione. (B) Mulliken charge distribution of (a) compound 1; benzoquinone, (b) compound 2; naphthalene-1,4-dione, and (c) compound 3; 2-isopropyl-5-methylcyclohexa-2,5-diene-1,4-dione.

spectrum of toxicity underscores that, while 2 may be a solid candidate for biological interactions.

Finally, molecular docking with the *CDK4*-Cyclin D3 complex (PDB 7SJ3). The compound 2 shows the strongest and consistent binding affinity (-7.4 kcal mol^{-1}), where the interaction involved a hydrogen bond and π-π stacking with significant residues including TRP A:179. This interaction mode is consistent with known *CDK4* inhibitors and confirms its high binding affinity to the kinase active site. Compound 3 would be found in moderate binding affinity (-6.8 kcal mol^{-1}) by hydrogen bonds with HIS A:95 and VAL A:96, implying a considerable but less strong interaction with the receptor. Compound 1 exhibits the weakest docking score (-5.7 kcal mol-1), however, it interacts through stabilizing hydrophobic and van der Waals contacts, which can retain its binding orientation fairly well.

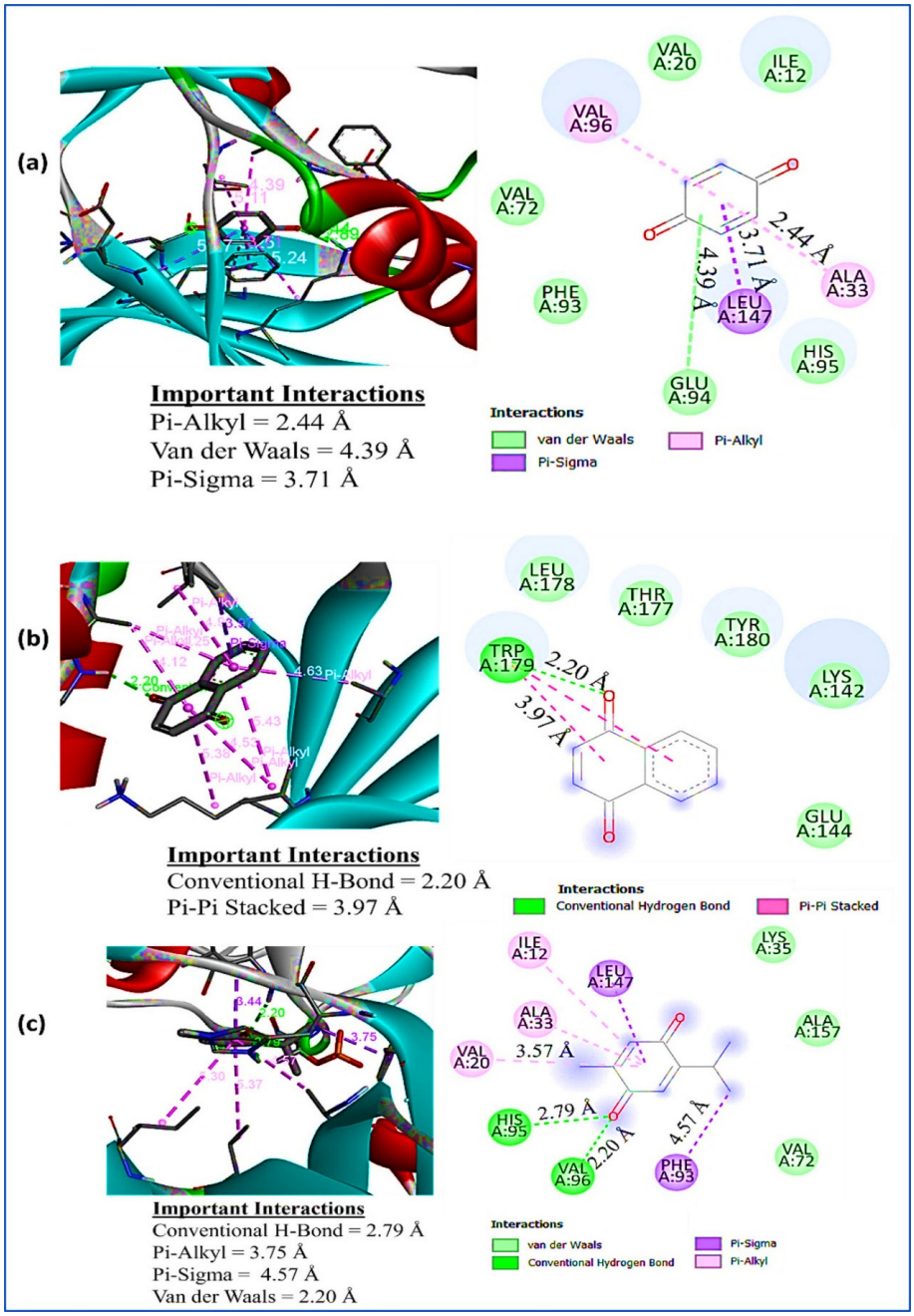

Figure 4: Docked structure of (a) compound 1 (benzoquinone), (b) compound 2 (naphthalene-1,4-dione), and (c) compound 3 (2-isopropyl-5-methylcyclohexa-2,5-diene-1,4-dione) with 7SJ3 receptor (3D docked view, interactions with bond lengths and 2D interaction diagram).

CONCLUSION

A series of chemical compounds, including *benzoquinone, naphthalene-1,4-dione* and *2-isopropyl-5-methylcyclohexa-2,5-diene-1,4-dione*, were studied by the quantum chemical calculation method, ADMET prediction and molecular docking. The FMO calculation and DOS analysis showed that compound 3 is more chemically reactive, with the narrowest energy gap, while compound 2 is relatively stable. MEP mapping confirmed that carbonyl oxygens are the dominant reactive sites, with compound 3 showing the highest electronegative potential. ADMET results indicated that compound 1 is highly soluble with good BBB penetration, compound 2 has strong CYP inhibition but higher mutagenicity and liver toxicity risk, and compound 3 is more lipophilic with wider tissue distribution but poor CNS penetration. Docking studies showed compound 2 to be the strongest binder to *CDK4*-Cyclin D3 (-7.4 kcal/mol) via stable hydrogen bonding and π-π stacking with TRP A:179, while compound 3 demonstrated moderate binding stabilised by hydrogen bonds and hydrophobic interactions. Inclusive, compound 2 stands out as the most hopeful *CDK4/6* inhibitor scaffold despite toxicity apprehensions, whereas compound 3 offers balanced reactivity and binding possible, and compound 1, though safer in some respects, exhibits weaker binding affinity.

ACKNOWLEDGEMENT

This work was funded by the University of Jeddah, Jeddah, Saudi Arabia, under grant No. (UJ-25-DR-3288). Therefore, the author thanks the University of Jeddah for its technical and financial support.

ABBREVIATIONS

CDK: Cyclin-Dependent Kinase; **SAR:** Structure activity relationships; **ROS:** Reactive oxygen species; **DOS:** Density of states; **Rb:** Retinoblastoma; **ADMET:** Absorption, Distribution, Metabolism, Excretion, and Toxicity; **FMO:** Frontier Molecular Orbital; **MEP:** Molecular Electrostatic Potential; **H-HT:** Hepatotoxicity; **DILI:** Drug-induced liver injury; **FDAMDD:** FDA maximum daily dose.

CONFLICT OF INTEREST

The authors declare that there is no conflict of interest.

FUNDING

This work was supported by funding under grant UJ-25-DR-3288.

SUMMARY

Benzoquinone derivatives were evaluated via DFT, ADMET, and docking to CDK4 Cyclin D3: compound 3 was most reactive, while compound 2 showed the best binding (-7.4 kcal/mol; H-bonds/π-π with TRP A:179) but higher toxicity risk. Overall, compound 2 is the top CDK4/6 scaffold, with compound 3 moderate and compound 1 weakest.

REFERENCES

Abdelmonsef, A. H., El-Naggar, M., and Ibrahim, A. O. A. (2024). Computational ADMET prediction and toxicity assessment of quinazolin-2,4-dione derivatives. Molecules, 29(23), 5529.

Abuhejail, R. M., Radwan, A. A., Alzoman, N. Z., and Darwish, I. A. (2024). Formation and characterization of charge transfer complex between alectinib and 2,3-dichloro-5,6-dicyano-1,4-benzoquinone: Application to development of microwell spectrophotometric method. Sustainable Chemistry and Pharmacy, 39, 101524.

Allouche, A.-R. (2012). Gabedit: A graphical user interface for computational chemistry softwares. Journal of Computational Chemistry, 32, 174-182.

Asghar, U., *et al.* (2015). The history and future of targeting cyclin-dependent kinases in cancer therapy. Nature Reviews Drug Discovery, 14(2), 130-146.

Azevedo, W. F., de. (2011). Molecular dynamics simulations of cyclin-dependent kinases. Journal of Molecular Modeling, 17(5), 1129-1137.

Becke, A. D. (1993). Density-functional thermochemistry. III. The role of exact exchange. Journal of Chemical Physics, 98, 5648-5652.

BIOVIASystemes, Dassault. (2021). BIOVIA Discovery Studio. San Diego: Dassault Systemes.

Cavallo, G., Metrangolo, P., Milani, R., Pilati, T., Priimagi, A., Resnati, G., and Terraneo, G. (2016). The halogen bond. Chemical Reviews, 116(4), 2478-2601.

Cristaldi, G., and De Proft, F. (2022). Density functional theory, chemical reactivity, and the Fukui functions. Foundations of Chemistry, 24, 59-71.

Dennington, R., Keith, T. A., and Millam, J. M. (2016). GaussView, Version 6.1. Semichem Inc., Shawnee Mission, KS.

El-Helw, EAE., *et al.* (2024). Synthesis and *in silico* studies of certain benzo[f]quinoline-based heterocycles as antitumor agents. Scientific Reports, 14(1), 15522.

Ferreira, L. G., dos Santos, R. N., Oliva, G., and Andricopulo, A. D. (2015). Molecular docking and structure-based drug design strategies. Molecules, 20(7), 13384-13421.

Frisch, M. J., Pople, J. A., and Binkley, J. S. (1984). Self-consistent molecular orbital methods. 25. Supplementary functions for Gaussian basis sets. Journal of Chemical Physics, 80, 3265-3269.

Frisch, M. J., Trucks, G. W., Schlegel, H. B., *et al.* (2016). Gaussian 16, Revision A.03. Gaussian, Inc., Wallingford CT.

Gu, J., Wang, T., Song, Y., and Ma, J. (2024). Catalysis of first triplet p-benzoquinone for electron ejection from sulfite: Significance of single electron transfer. Chemical Engineering Journal, 494, 152962.

Guan, L., Yang, H., Cai, Y., Sun, L., Di, P., Li, W., Liu, G., and Tang, Y. (2018). ADMET-score: A comprehensive scoring function for evaluation of chemical drug-likeness. MedChemComm, 10(1), 148-157.

Krishna, K. M. (2024). Possible NLO response and electrical/charge transfer capabilities of natural anthraquinones as p-type organic semiconductors: A DFT approach. Journal of Molecular Modeling, 30.

Kumar, R., Kar, R., and Maity, D. K. (2025). Accurate prediction of HOMO-LUMO gap using DFT functional and application to next generation organic telluro[n]helicenes materials. Journal of Computational Chemistry, 46(18), e70175.

Lee, C., Yang, W., and Parr, R. G. (1988). Development of the Colle Salvetti correlation-energy formula into a functional of the electron density. Physical Review B, 37, 785-789.

Li, F., Shi, S., Yi, J., Wang, N., He, Y., Wu, Z., Peng, J., Deng, Y., Wang, W., Wu, C., Lyu, A., Zeng, X., Zhao, W., Hou, T., and Cao, D. (2024). ADMETlab 3.0: An updated comprehensive online ADMET prediction platform enhanced with broader coverage, improved performance, API functionality and decision support. Nucleic Acids Research, 52(W1), W422-W431.

Li, H., Wang, T., and Zhao, G. (2025). Molecular dynamics simulation of CDK2 complexes with small molecule inhibitors: Stability and conformational analysis. Journal of Chemical Information and Modeling, 65(7), 2134-2145.

Malumbres, M., and Barbacid, M. (2009). Cell cycle, CDKs and cancer: A changing paradigm. Nature Reviews Cancer, 9(3), 153-166.

Meng, X. Y., *et al.* (2011). Molecular docking: A powerful approach for structure-based drug discovery. Current Computer-Aided Drug Design, 7(2), 146-157.

Rezvan, V. H., and Salehzadeh, J. (2025). Exploring charge transfer complexes of fluoroquinolone drugs and π-acceptors (picric acid and 3,5-dinitrobenzoic acid): DFT insights into electronic interactions, thermodynamic stability, FMOs, and NLO properties. Chemistry Select, 10.

Santos, R., *et al.* (2017). A comprehensive map of molecular drug targets. Nature Reviews Drug Discovery, 16(1), 19-34.

Sharma, M., Savita, S., Wadhwa, K., Mishra, V., Javed, S., Ranjan, K. R., Rathi, A. K., and Kaur, H. (2025). Experimental, spectroscopic analysis, DFT and molecular docking studies of pyridine-based biologically active anti-fungal drug derivative of para-benzoquinone and benzimidazole. Journal of Molecular Structure, 1338, 142212.

Sofi, S., Mehraj, U., Qayoom, H., Aisha, S., Almilaibary, A., Alkhanani, M., and Mir, M. A. (2022). Targeting cyclin-dependent kinase 1 (CDK1) in cancer: Molecular docking and dynamic simulations of potential CDK1 inhibitors. Medical Oncology, 39(9), 133.

Solanki, P. (2023). A comprehensive analysis of the role of molecular docking in the development of anticancer agents against the cell cycle CDK enzyme. Biocell, 47(4), 707-729.

Trott, O., and Olson, A. J. (2009). AutoDock Vina: Improving the speed and accuracy of docking with a new scoring function, efficient optimization, and multithreading. Journal of Computational Chemistry, 31(2), 455-461.

Valarmathi, T., Premkumar, R., Jebaseelan, J., and Franklin, M. (2023). Spectroscopic characterization, quantum chemical and molecular docking studies on 1-chloroanthraquinone: A novel oral squamous cell carcinoma drug. Polycyclic Aromatic Compounds, 44, 1816-1834.

White, N. J., *et al.* (2025). Benzoquinone, 1,4 naphthoquinone radical anions, and their didehydro derivatives: Electroanalytical and predicted negative ion photoelectron spectroscopic studies. Physical Chemistry Chemical Physics, 27, 8976-8993.

Xiong, G., Wu, Z., Yi, J., Fu, L., Yang, Z., Hsieh, C., Yin, M., Zeng, X., Wu, C., Lu, A., Chen, X., Hou, T., and Cao, D. (2021). ADMETlab 2.0: An integrated online platform for accurate and comprehensive predictions of ADMET properties. Nucleic Acids Research, 49(1), W5-W14.

Zheng, L., Yang, Y., and Bao, J. (2022). Discovery of novel inhibitors of CDK2 using docking and physics-based binding free energy calculation. Chemical Biology and Drug Design.

Cite this article: Hakeem IJ. *In silico* Study toward Electronic Structures of Bioactive Compounds Benzoquinone and its Derivatives: Toxicity and Molecular Docking against Cyclin-Dependent Kinase. Int. J. Pharm. Investigation. 2026;16(4):1479-88.